Potassium Carbonate to Unlock a GaCl 3 -Catalyzed C-H Propargylation of Arenes

Marie Vayer, Sophie Rodrigues, Solène Miaskiewicz, David Gatineau, Yves Gimbert, Vincent Gandon, Christophe Bour

Potassium Carbonate to Unlock a $GaCl_3$-Catalyzed C–H Propargylation of Arenes

Marie Vayer,[†,#] *Sophie Rodrigues,*[†,#] *Solène Miaskiewicz,*[†] *David Gatineau,*[ξ] *Yves Gimbert,*[ξ,§] *Vincent Gandon**[,†,‡] and *Christophe Bour**[,†]

[†]Institut de Chimie Moléculaire et des Matériaux d'Orsay (ICMMO), CNRS UMR 8182, Université Paris-Saclay, Bâtiment 420, 91405 Orsay cedex, France.

[‡]Laboratoire de Chimie Moléculaire (LCM), CNRS UMR 9168, École Polytechnique, Institut Polytechnique de Paris, route de Saclay, 91128 Palaiseau cedex, France.

[ξ]Univ. Grenoble Alpes, CNRS, DCM, 38000 Grenoble, France

[§]Sorbonne Université, CNRS, Institut Parisien de Chimie Moléculaire, IPCM, Paris 75005, France.

[#]These authors contributed equally.

KEYWORDS. allenes, C–H propargylation, DFT computations, gallium, kinetic study

ABSTRACT. A gallium-catalyzed C–H propargylation of arenes using bromoallenes is described. The development of this new reaction was first hampered by a side hydroarylation process catalyzed by adventitious protons, easily generated from the solvent (1,2-dichloroethane).

This hidden Brønsted acid catalysis could be bypassed by using K_2CO_3 as insoluble base. The unexpected compatibility of this base with the Lewis acid catalyst $GaCl_3$ allowed a strictly gallium-catalyzed process that was thoroughly studied by kinetics, ^{71}Ga NMR experiments and DFT computations. The $GaCl_3/K_2CO_3$ system triggers the C–H propargylation of a wide range of arenes and heteroaromatics using a variety of bromoallenes.

INTRODUCTION. Organic synthesis greatly relies on catalytic processes, a large part of which involving Lewis acids. This covers a wide range of transformations, including industrially relevant ones such as aldol, Friedel-Crafts, Mannich, Michael reactions, coupling reactions, etc. The field of Lewis-acid catalyzed homogeneous transformations is still a thriving area of research in which impressive progress is frequently reported. The quest for the true active species in these reactions is also still actively pursued, and often offers many surprises. For instance, the role of superelectrophilic species,[1] i.e. Lewis acids activated by themselves or other electrophilic species,[2] has been disclosed in some reactions such as the carbonyl-olefin metathesis,[3,4] the Friedel-Crafts alkylation,[5] the Diels-Alder cycloaddition[6] or the transfer hydrogenation of alkenes.[4] In addition to such unexpected associations of metals and ligands, the active species can be formed more insidiously (Scheme 1). For instance, decomposition processes may generate a new Lewis acid from the counterions of the introduced complex, a phenomenon that one could call *hidden Lewis acid catalysis*.[7] Another decomposition pathway that can take place with strong Lewis acids is the formation of Brønsted acids, notably superacids, from traces of water, from the solvent or from the ligands. These proton donors may act as the true active species, a phenomenon referred to as *hidden Brønsted catalysis*.[8]

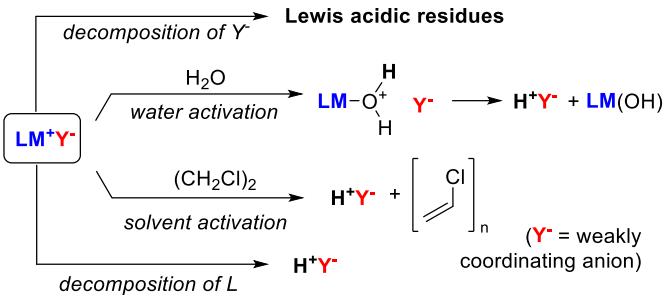

Scheme 1. Possible Decomposition Pathways Leading to the Real Active Species.

Some tests based on the selectivity of catalytic reactions,[9] on the loss of activity,[10] or on the formation of colored cations,[11] have been developed to reveal the Lewis or Brønsted acidity under given experimental conditions. What remains more common is a blank test with the Brønsted acid corresponding to the Lewis acid used (e.g. HOTf or $HNTf_2$ if $M(OTf)_n$ or $M(NTf_2)_n$ have been employed), or the use of a proton scavenger such as 2,6-di-*tert*-butylpyridine (DTBP), expected to catch only protons and not metals due to its steric hindrance.[12] However, these tests can be flawed for many reasons: (*i*) the selectivity of these Brønsted acid-catalyzed processes can be indistinguishable from that expected for metal-catalyzed pathways,[13,14] (*ii*) proton scavengers can trap metal ions by forming an out-of-plane σ-complex (Scheme 2, Eq 1),[7a,15] or react with a chlorinated solvent, leading to the deactivation of the Lewis acid (Scheme 2, Eq 2)[7a], and *iii*) their protonated forms might also be active catalysts.[16]

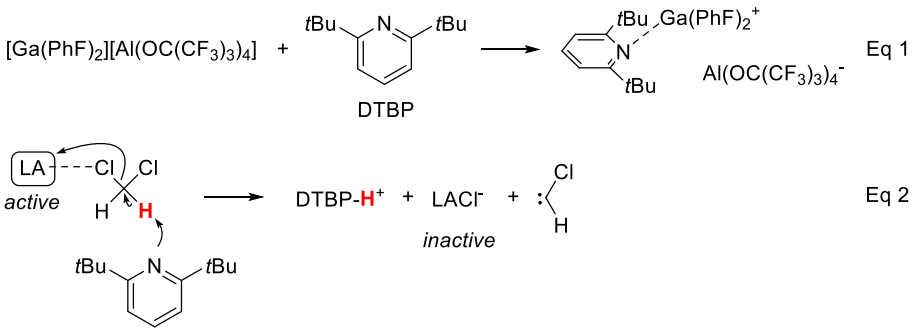

Scheme 2. Direct and Indirect Deactivation of the Catalyst by DTBP.

During our studies on gallium-catalyzed reactions,[4,5,9b,17] we have often been confronted to this dilemma and the difficulty to develop univocal reaction conditions that would allow the Lewis acid to express its true nature. We assumed that, since the presence of a hidden acid is always a source of questioning, the use of a weakly-soluble base that would not interact with the Lewis acid nor perturb the catalytic cycle would allow a true metal-catalyzed event. This strategy was applied in this study, in which we show how the C–H propargylation of arenes with bromoallenes can be performed in the presence of a catalytic amount of $GaCl_3$ in 1,2-dichloroethane (1,2-DCE), as long as the insoluble base K_2CO_3 is present in the medium (Scheme 3, Eq 3). In the absence of the base, a hidden-proton-catalyzed hydroarylation of the allene prevails. With a soluble base, even a hindered one such as DTBP, no reaction takes place.

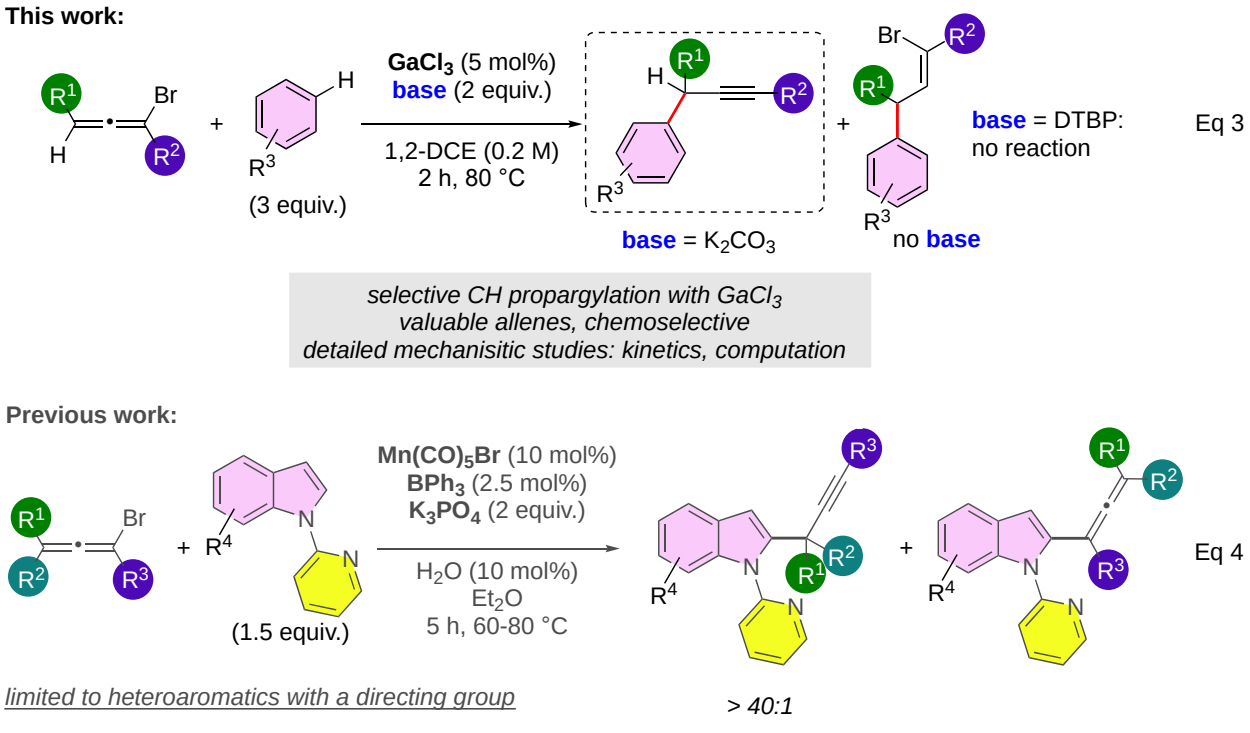

Scheme 3. Gallium-Catalyzed C–H Propargylation of Bromoallenes.

The C–H propargylation of arenes is a reaction of great interest, allowing the direct introduction of an easily transformable alkyne moiety[18] through the formation of a Csp^2–Csp^3 bond.[19] In contrast with C–H allylations, which have been reported under various transition metal-catalyzed conditions and others,[20] the C–H propargylation of arenes has been much less studied. In most cases, the coupling partner is a propargylic alcohol,[21] or an alkyne exhibiting a leaving group at the propargylic position, but avoiding the S_N2' process leading to an allene[22] instead of the alkyne has been rarely achieved.[23] Interestingly, Glorius and co-workers have recently shown that bromoallenes could be used for the direct C–H propargylation of arenes under manganese(I)/Lewis acid co-catalysis (Scheme 3, Eq 4).[24] Usually, allenes exhibiting a leaving group lead to C–H allenylation products with arenes,[25] but using $Mn(CO)_5Br$ as precatalyst, BPh_3 to strengthen the electrophilicity of the bromoallene and traces of water to improve the solubility of the base (K_3PO_4), virtually suppressed the formation of the arylallene. While efficient, this method is limited to 2-pyridylindoles and 2-pyridylpyrroles as arene partners.

Even though present in a variety of biologically active molecules,[26] bromoallenes still represent an underdeveloped class of reagents in organic chemistry.[27] We recently reported a new synthetic approach towards such compounds by electrophilic bromination of 7-alkynylcycloheptatrienes[28] and their use in different coupling reactions. We then envisioned broadening their application in direct C–H propargylation by avoiding hidden Brønsted catalysis. Herein, we disclose our findings regarding the in-depth study on this reaction based on a kinetic study and DFT computations, as well as its applicability to a wide range of substrates in a very efficient way.

RESULTS AND DISCUSSION.

We began our study by probing different catalytic systems towards the reaction of bromoallene **1a** and anisole (Table 1). With $GaCl_3$ as Lewis acid (5 mol%) in 1,2-DCE at 80 °C for 2 h, we observed the *p*-allylation product **3aa** instead of the C–H propargylation product **2aa** (Entry 1). While clearly identified as the major component of the mixture, **3aa** could not be separated from impurities. It became possible to isolate it in pure form using $ZnBr_2$ (Entry 2). Lower reactivity and decomposition were respectively observed with the corresponding chloro- or iodoallene (see the Supporting Information, Table S7)The same allylation product was isolated in good yield using HOTf or $HNTf_2$ as catalyst (Entries 3 and 4). We thus supposed that under such reaction conditions, **3aa** was the result of a protocatalyzed reaction, meaning hidden Brønsted catalysis with $GaCl_3$ and $ZnBr_2$. Several bases were tested to avoid this protocatalysis (2 equiv, Entry 5). The soluble bases *t*BuOK, Et_3N and DTBP quenched the reactivity, but it could be due to the formation of a donor-acceptor complex trapping the Lewis acid, even with DTBP with which one can expect the formation of an out-of-plane σ-complex, as shown in Scheme 2, Eq 1. DFT calculations support this scenario with DTBP and $GaCl_3$, the corresponding solvent-corrected free energy being -15.8 kcal/mol (see the Supporting Information, Scheme S1). Poorly soluble carbonates were then tested (Entries 6-8). A complete change of selectivity in favor of the C–H propargylation product **2aa** was observed with Li_2CO_3, Na_2CO_3 and K_2CO_3. With the latter, an excellent yield of 90% was obtained.[29] Gratifyingly, the reaction could be scaled up to 2 mmol without affecting the yield (87%, 0.47 g) (Entry 9). On the other hand, the more soluble base Cs_2CO_3 led to a lower conversion and a poor **2aa**/**3aa** selectivity (Entry 10). Using $NaHCO_3$, full conversion was reached, but **3aa** was obtained as the major product (Entry 11). Lastly, with

K_3PO_4, the conversion was limited to 68% (Entry 12). Potassium carbonate was thus chosen as the best base and other factors were next screened. Having verified that the metal catalyst was mandatory, we tested various Lewis acids of the Group 13 series (B, Al, Ga, In) and also Fe, Ag, Au and Zn salts (see the Supporting Information, Tables S1-2). The best of this series was actually $ZnBr_2$, but it is not as selective as $GaCl_3$.[30] Going back to $GaCl_3$, lowering the proportion of K_2CO_3 lowered the selectivity (Entries 13 and 14). Regarding the reaction media, while dichloromethane and toluene proved compatible with the title transformation (Entries 15 and 16), all strongly coordinating solvents prevented the reaction (Entry 18). Importantly, in toluene, a solvent in which less protons are released than in a chlorinated one,[9b] the C–H propargylation works without an external base, but the selectivity is not as high as in 1,2-DCE (Entry 17).

Table 1. Optimization of the Reaction Conditions.

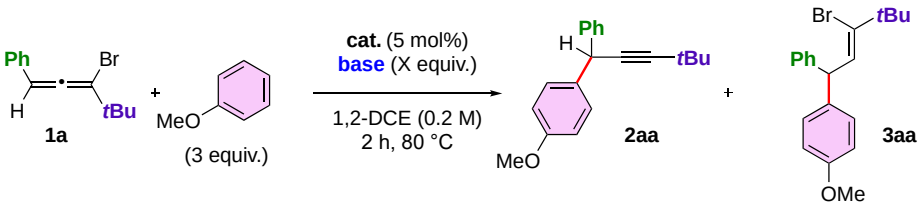

Entry	Cat.	Base	X	Conv. [%]	Ratio 2aa/3aa	Yield 2aa [%][a]
1	$GaCl_3$	-	-	100	0/1	-[b]
2	$ZnBr_2$	-	-	100	0/1	67
3	HOTf	-	-	100	0/1	73
4	$HNTf_2$	-	-	100	0/1	83
5	$GaCl_3$	*t*BuOK, Et_3N, or DTBP	2	0	-	-
6	$GaCl_3$	Li_2CO_3	2	100	1/0	45[c]

7	$GaCl_3$	Na_2CO_3	2	100	1/0	30
8	**$GaCl_3$**	**K_2CO_3**	**2**	**100**	**1/0**	**90**
9	$GaCl_3$	K_2CO_3	2	100	1/0	87[d]
10	$GaCl_3$	Cs_2CO_3	2	71	59/41	-
11	$GaCl_3$	$NaHCO_3$	2	100	44/66	96
12	$GaCl_3$	K_3PO_4	2	68	90/10	-
13	$GaCl_3$	K_2CO_3	1	100	83/17	81
14	$GaCl_3$	K_2CO_3	0.2	100	41/59	-
15	$GaCl_3$	K_2CO_3	2	100	1/0	90[e]
16	$GaCl_3$	K_2CO_3	2	100	1/0	75[f]
17	$GaCl_3$	-	2	100	57/43	88[f]
18	$GaCl_3$	K_2CO_3	2	-	-	-[g]

[a] Yields of isolated **2aa**. [b] Not separable from impurities. [c] Not pure. [d] Reaction on a 2 mmol scale. [e] Reaction performed in DCM at 40 °C. [f] Reaction performed in toluene. [g] Reaction performed in Et_2O, THF, AcOEt, DMF or 1,4-dioxane.

To the best of our knowledge, this is the first time that $GaCl_3$ is used jointly with a Brønsted base in a catalytic transformation. We should also point out that this method is complementary to that reported by Glorius,[24] since the Mn(I)/BPh_3 catalytic system is inactive with, for instance, anisole (Scheme 4, Eq 5). Clearly, the allylation product **3aa** is not an intermediate towards the propargylation product **2aa**, as shown in Eq 6. It seems also clear that K_2CO_3 acts as a buffer in this system, as introducing a soluble proton source such as pivalic acid dramatically lowered the yield (Eq 7).

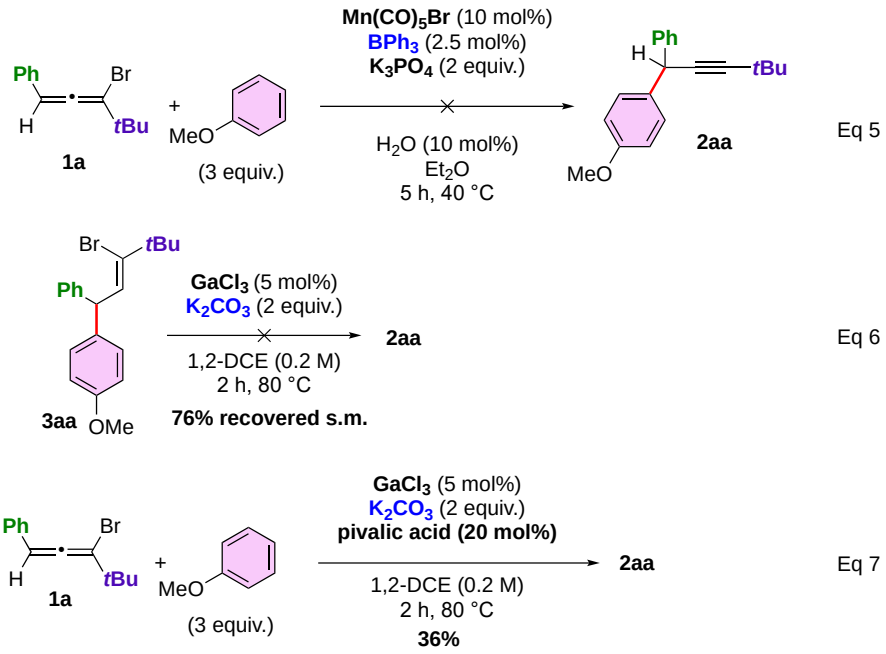

Scheme 4. Control Experiments.

Subsequently, we tested the versatility of the catalytic system with respect to different arenes and bromoallenes **1** (Scheme 5). The tested arenes proved to be effective coupling partners, in spite of the electronic effects at the *ortho*-, *meta*-, and *para*-positions (**2ab-2aj**). We were also pleased to see that variously substituted phenols were exclusively propargylated at the *para* or *ortho* position (**2ak-2an**, 78-93%). The reaction sequence is not limited to phenyl nucleophiles but could be also extended to heteroaromatics displaying indenyl, pyrrolyl, furyl or thienyl groups, delivering **2ao-2au** with usually good regioselectivities. The substituents on the allene **1** are also not limited to *tert*-butyl and phenyl groups. Trisubstituted allenes bearing electron-poor or electron-rich arenes, as well as alkyl groups, proved compatible with the gallium-catalyzed C–H propargylation (**2ba-2ia)**.

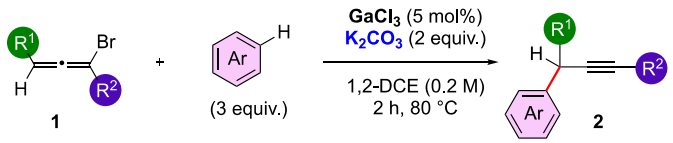

Variation of aromatic nucleophiles (isolated yield)

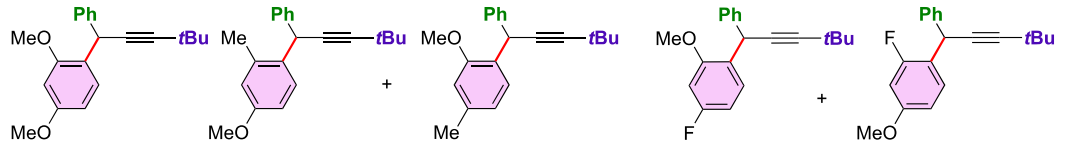

2ab, 85% **2ac/2ac'** (50/50), 67% **2ad/2ad'** (63/37), 79%[a]

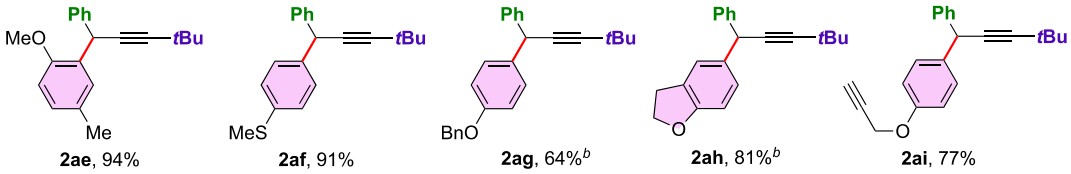

2ae, 94% **2af**, 91% **2ag**, 64%[b] **2ah**, 81%[b] **2ai**, 77%

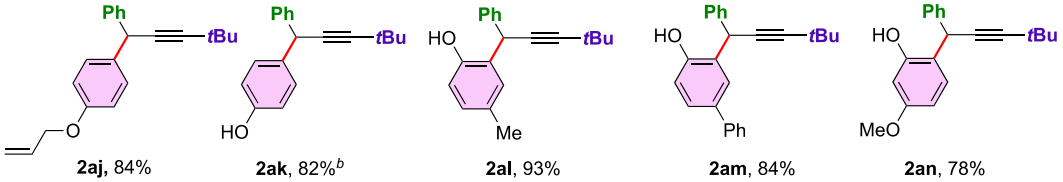

2aj, 84% **2ak**, 82%[b] **2al**, 93% **2am**, 84% **2an**, 78%

Variation of heteroaromatic nucleophiles

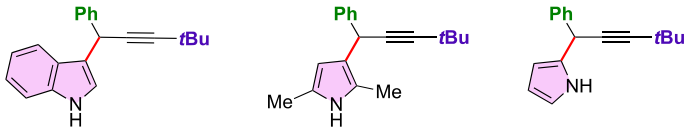

2ao, 90% **2ap**, 66% **2aq**, 63%

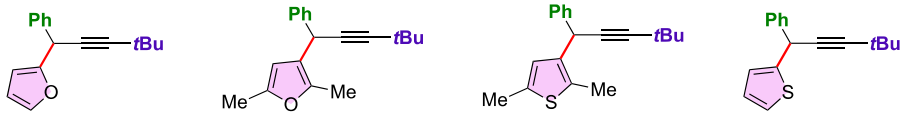

2ar, 50% **2as**, 91% **2at**, 76% **2au**, 47%[c]

Variation of allenes

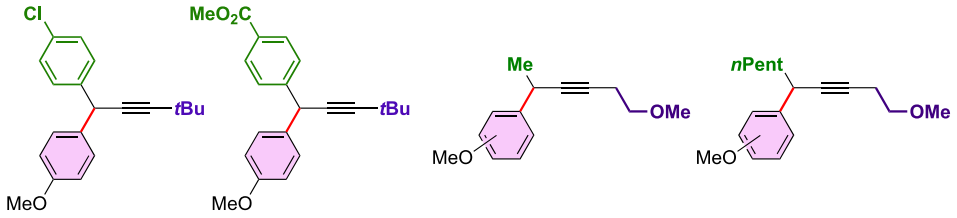

2ba, 82% **2ca**, 79% **2da**, 45% (*p*/*o* 55/45) **2ea**, 53% (*p*/*o* 70/30)

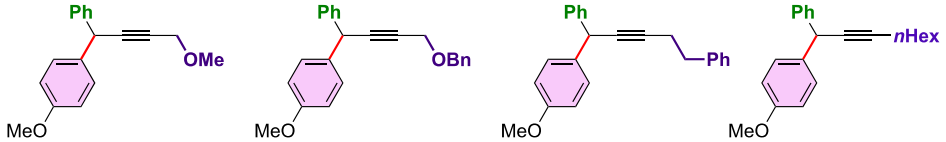

2fa, 86% **2ga**, 72% **2ha**, 74% **2ia**, 60%

[a]Reaction performed at 40 °C, 72 h. [b]Reaction performed at 25 °C, 24 h. [c]34% yield of the hydroarylation product also isolated (see SI)

Scheme 5. Scope of Arenes and Bromoallenes.

Some incompatible substrates are indicated in the Supporting Information, Chart S1. Of note, the 2-pyridylindole used by Glorius *et al*[24] (Scheme 3, Eq 4, R^4 = H) is not reactive under our conditions.

To shed light on the mechanism of the C–H propargylation process, additional experiments were performed (Scheme 6). First, the reaction of the enantioenriched bromoallene **1e** is accompanied by a great loss of the stereochemical information (Eq 8), which suggests a cationic mechanism. Of note, the allene is configurationally stable under the reaction conditions without any decomposition (Eq 9, *ee* determined by chiral HPLC). Stoichiometric reactions were monitored by ^{71}Ga NMR in CD_2Cl_2 (Eqs 10 and 11). $GaCl_3$ was observed as a broad peak at 220 ppm, and no significant change apart from further broadening was observed after adding K_2CO_3 (Eq 10). Either with or without the base, adding substrate **1a** promoted an immediate change of the ^{71}Ga NMR spectrum, showing sharp peaks between 0 and 187 ppm, which are typical of the presence of $GaCl_4^-$, $GaCl_3Br^-$, $GaCl_2Br_2^-$, $GaClBr_3^-$ and $GaBr_4^-$.[31] This suggests an abstraction of Br^- from **1a** to generate $GaCl_3Br^-$, which undergoes ligand redistribution. Addition of anisole to this mixture did not change the spectrum. DFT computations indicate that the coordination of the bromoallene to $GaCl_3$ or 0.5 Ga_2Cl_6 is a favorable process (-11.1 or -3.3 kcal/mol), as is the formation of an ion pair (-2.2 kcal/mol, i.e. -13.3 kcal/mol from **1a** and $GaCl_3$) (Eq 12). Conductometry was used to corroborate the dissociation of Br^- of **1a** in the presence of $GaCl_3$ and K_2CO_3 (see the Supporting Information, Figures S11-12). The conductivity increases linearly with the **1a** concentration, indicating almost complete dissociation into ions.

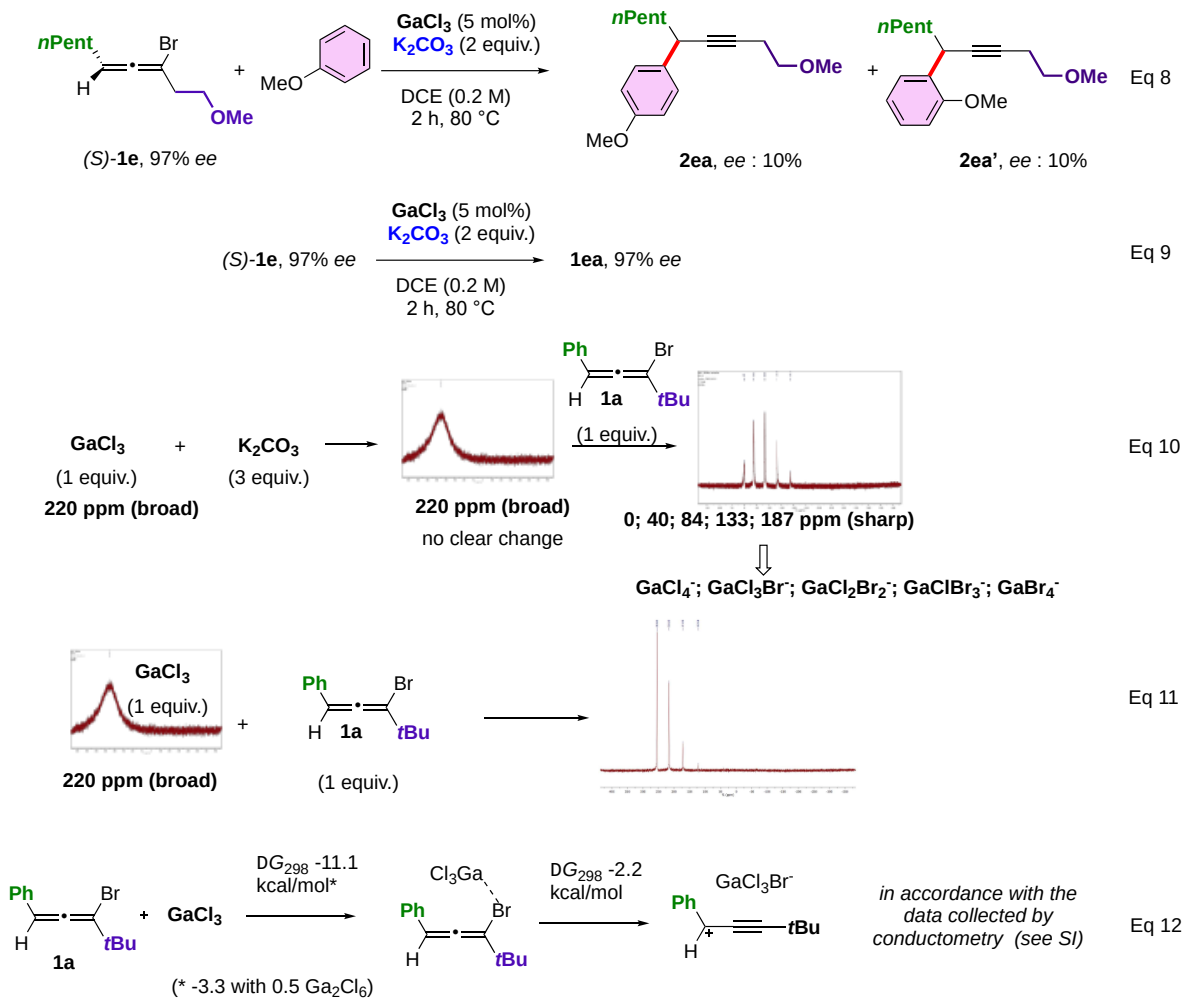

Scheme 6. Mechanistic Experiments.

KINETIC STUDY

As a further step to delineate the mechanism, we performed a reaction monitoring by ^{1}H NMR with an internal standard with stirring of the NMR tube at a spin rate of 50 Hz (Figure 1, left). If not stirred efficiently, the formation of the hydroarylation product **3aa** (marked in blue) was observed in addition to the minor C–H propargylation product **2aa** (marked in red) without any decomposition of the substrate (Figure 1, right). This further confirms that if the insoluble base is

not efficiently dispersed into the reaction medium, the neutralization of the adventitious Brønsted acid is not efficient and the protocatalytic pathway prevails.

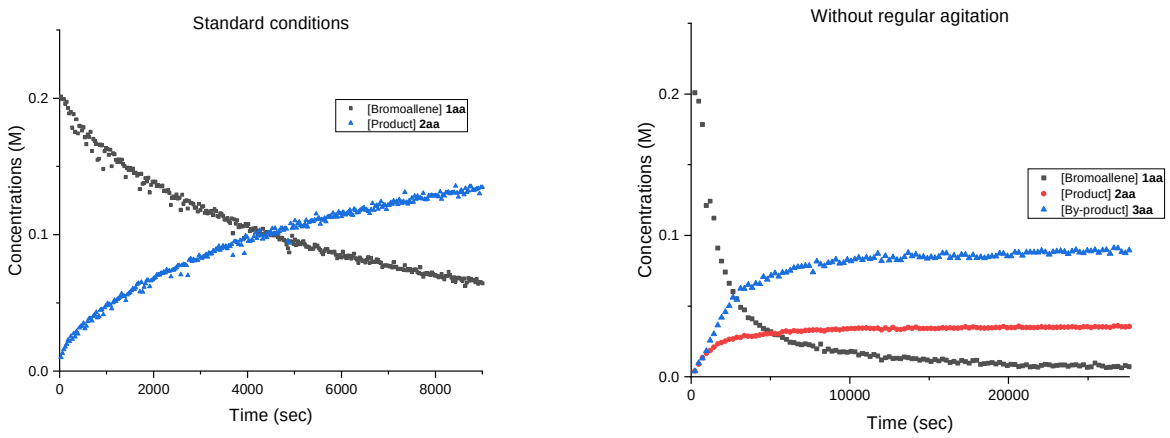

Figure 1. ^{1}H NMR spectroscopic monitoring of the reaction of **1aa** (0.12 mmol) with anisole (0.36 mmol) in the presence of K_2CO_3 (0.24 mmol) and $GaCl_3$ (5 mol%) at 20 °C in CD_2Cl_2 with (**left**) and without regular stirring (**right**).

Subsequent efforts were devoted to a detailed kinetic study of the gallium-catalyzed C–H propargylation. When performed in the presence of a large excess (10 equiv) of anisole, an exponential decay was observed for the concentration profile of **1a**, consistently with a first-order with respect to **1a** with an apparent pseudo first-order rate constant of 4.6 10^{-4} s^{-1} (Scheme 7, see also the details of kinetic study in the Supporting Information, Figures S15-21). The reaction order in anisole was determined by varying its concentration.[32] When plotting the logarithm of the apparent rate constant against the logarithm of the concentration of anisole (from 3 to 8 equiv), the slope of the straight line indicated a negative order of -1.3 with respect to anisole. The kinetic data clearly showed the ability of the nucleophile to inhibit the catalytic efficiency of $GaCl_3$ (vide infra). From a set of kinetic experiments with a catalyst loading

varying within the synthetically relevant range (5−10 mol%), a half-order with respect to $GaCl_3$ was assessed using the VTNA method.[33] This result is consistent with the dissociation of Ga_2Cl_6 into $GaCl_3$ prior to the rate-determining step.

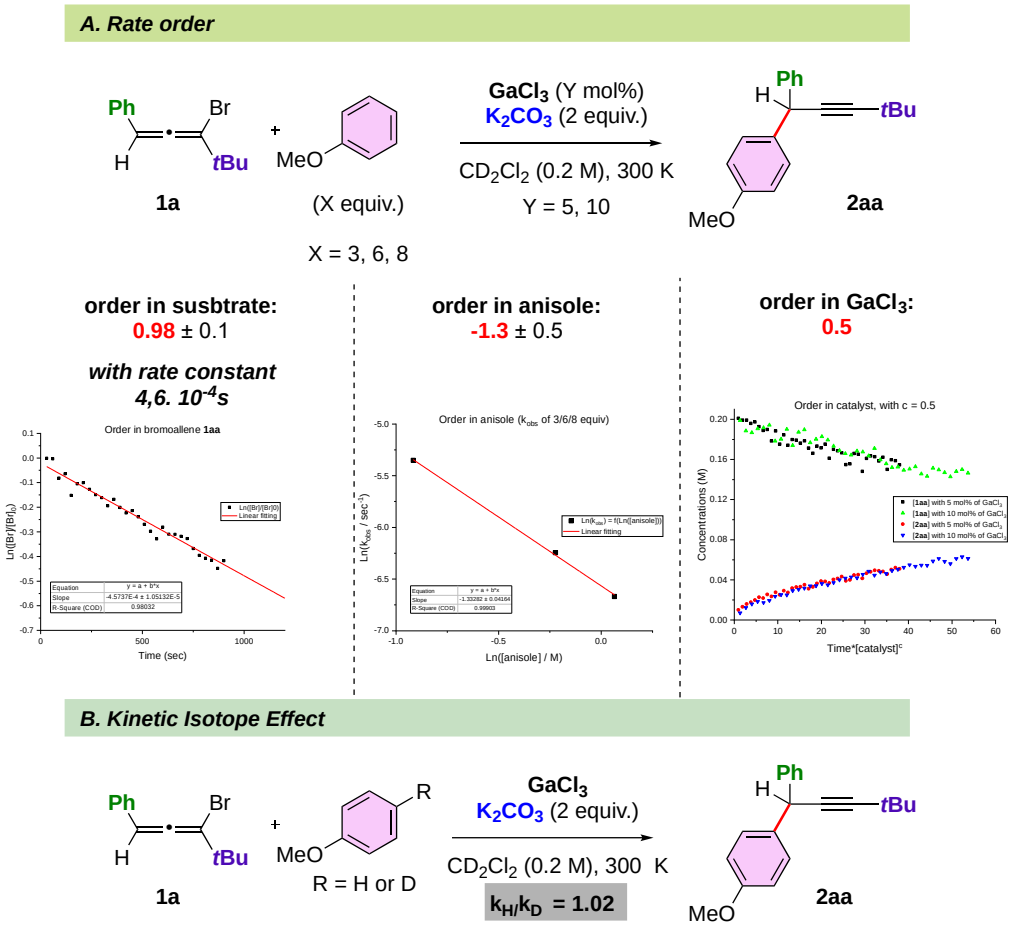

Scheme 7. Kinetic Investigations of the Gallium-Catalyzed C–H Propargylation of Arenes Based on the Consumption of the Substrate using three independent methods relying on "degeneration of order", "initial rate" and "normalized time scale method".

The approximately first order dependence of the reaction in substrate **1a** and half order in Ga suggest that bromine abstraction should be the rate-determining step rather than the addition of anisole on the putative propargyl cation. This was further confirmed by deuterium labelling

experiments, where minor kinetic isotope effect of k_H/k_D= 1.02 was observed, indicating that a C–H cleavage of the arene is not the rate-limiting step (see the Supporting Information).

DFT

To get more insight into the reaction mechanism, DFT computations were carried out using the Gaussian 09 software package.[34] Geometries of minima and transition states were optimized using the ωB97-XD[35] functional. The 6-31+G(d,p) basis set for selected all atoms.[36] The values presented are Δ*G* in kcal/mol at 298.15 K. They include solvation correction for 1,2-dichloroethane, obtained using the PCM method.[37] The results are summarized in Scheme 8. As a reference system (**REF**), we used 0.5 equiv of Ga_2Cl_6, which is the natural dimeric form of $GaCl_3$ in the solid state and in weakly polar solvents,[38,39] anisole and bromoallene **1a**. The steps corresponding to the dissociation of 0.5 Ga_2Cl_6 by anisole to form $GaCl_3{\cdot}(C_7H_8O)$ are provided in the Supporting Information (Figure S25). The highest-lying transition state of this stepwise dissociation was located at only 3.9 kcal/mol on the free energy surface. Computation of the bromine abstraction in the presence of anisole yielded $\mathbf{TS_{AB}}$, lying 6.0 kcal/mol above **REF**. It connects the adduct **A**, containing $GaCl_3{\cdot}(C_7H_8O)$ and the bromoallene, to the corresponding ion pair **B**, which is 3.8 kcal/mol more stable than **REF**.[40] Alternatively, **B** can be obtained after ligand exchange between anisole and the bromoallene to give **F**, lying at 0.6 kcal/mol. The corresponding transition state $\mathbf{TS_{FB}}$, found at 4.2 kcal/mol on the energy surface, is 1.8 kcal/mol more stable than $\mathbf{TS_{AB}}$. Attack of anisole to the propargyl cation was modeled through $\mathbf{TS_{BC}}$, providing the Wheland-type intermediate **C** at -7.0 kcal/mol. Its deprotonation could be promoted by K_2CO_3, with subsequent neutralization of the released proton by K_2CO_3. The kinetics of a proton elimination cannot be computed, but such a step would be highly exergonic, leading to **E** at -69.1 kcal/mol. The deprotonation could also be triggered by the carbonate ions.

Of note, optimizing **C** and CO_3^{2-} irremediably led to the barrierless formation of a C–O bond at the anisole *meta* carbon due to the easy 1,4-addition (see Eq 13).[41] The formation of the carbonate adduct **G** is markedly exergonic by 40.3 kcal/mol from **C**. The deprotonation can then be modeled, but the barrier to reach $\mathbf{TS_{GE}}$ is 28.2 kcal/mol, which seems difficult to surmount under the reaction conditions. Another possibility is that the deprotonation is triggered by the $GaCl_3Br^-$ counterion. In this case, either one chlorine or the bromine atom could serve as a base. Using the bromine atom, the deprotonation transition state $\mathbf{TS_{CD}}$ was located at 2.0 kcal/mol. With a chlorine atom, the corresponding transition state was found at 5.5 kcal/mol (not shown). In spite of the rearomatization of the anisole moiety, the formation of **D** is endergonic by 7.8 kcal/mol, which is due to the solvent effect in favor of the ion pair **C** (without taking the effect of the polar solvent into account, this step is actually exergonic by 2.4 kcal/mol, which in agreement with the fact that C–H propargylation is observed in weakly polar toluene in the absence of an external base).

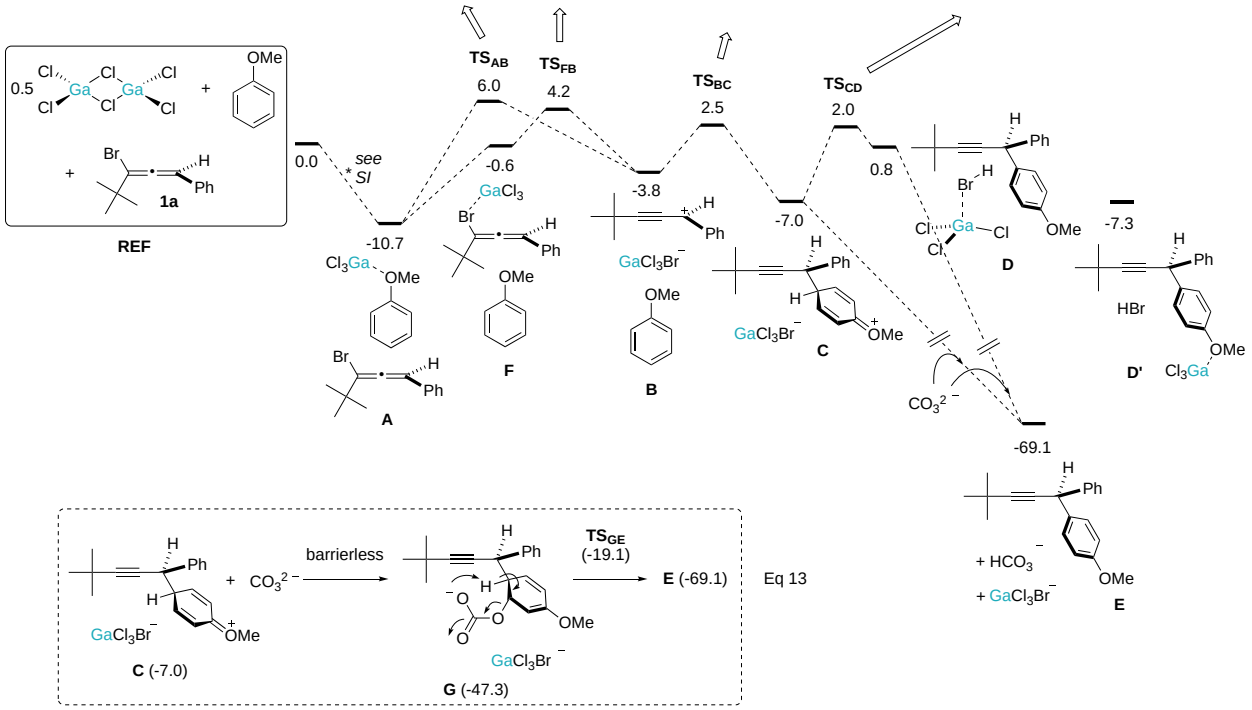

Scheme 8. Free Energy Profile (ΔG_{298}, kcal/mol) of the Gallium-Catalyzed C–H Propargylation of Anisole with Bromoallene **1a** (* see the Supporting Information for the dissociation of Ga_2Cl_6, Figure S25).

In the above mechanism, the rate-determining step (RDS) corresponds to the bromide abstraction. It is consistent with the finding of an order 1 in bromoallene. The 0.5 order in $GaCl_3$ is a good indicator that most of the catalyst is present as the inactive dimer Ga_2Cl_6 before the RDS.[33] Such species are indeed part of the computed dissociation of 0.5 Ga_2Cl_6 (see the Supporting Information, Figure S25, species **K** or **H**). Since anisole is not involved in the RDS, the low KIE of 1.02 is rationalized.[42] However, anisole has a detrimental effect on the reaction rate due to catalyst trapping.

CONCLUSION. Chlorinated solvents are often the most efficient ones for Lewis-acid catalyzed transformations, but the easy formation of protons can promote side reactions or decomposition. In the present case, we have found that the use of K_2CO_3 as an insoluble base is compatible with a $GaCl_3$-catalyzed transformation that works best in 1,2-DCE, but which follows a proton-catalyzed pathway in its absence. By bypassing hidden Brønsted catalysis, this strategy allowed to develop a truly Lewis acid-catalyzed C–H propargylation of arenes using bromoallenes, which is complementary to a transition-metal catalyzed reaction. The reaction is compatible with a large range of substrates. Kinetic, ^{71}Ga NMR and DFT studies pointed out the dissociation of the Ga_2Cl_6 dimer by the arene nucleophile and the formation of an ion pair from the bromoallene and monomeric $GaCl_3$ unit by Br^- abstraction (rate determining step). Attack of the propargyl cation by the arene and deprotonation of the Wheland-type intermediate then provides the C–H propargylation product. The unexpected compatibility of K_2CO_3 with $GaCl_3$ that we disclosed in this work represents a great opportunity to develop new and truly gallium-catalyzed transformations.

ASSOCIATED CONTENT

Supporting Information. Experimental procedures, characterization data, NMR spectra, additional experiments, Cartesian coordinates and total energies for all optimized geometries are given in the Supporting Information (PDF).

AUTHOR INFORMATION

Corresponding Authors

* Email: vincent.gandon@universite-paris-saclay.fr; christophe.bour@universite-paris-saclay.fr

Author Contributions

The manuscript was written through contributions of all authors. All authors have given approval to the final version of the manuscript.

Notes

The authors declare no competing financial interest.

ACKNOWLEDGMENT

We are grateful to Dr. Laurence Grimaud (Sorbonne Université) for helpful discussion. We thank the MESR, UPSaclay, Ecole polytechnique, and ANR-18-CE07-0033-01 (HICAT) for financial support. This work was granted access to the HPC resources of CINES under the allocation 2020-A0070810977 made by GENCI.

REFERENCES

1 a) Olah, G. A. Superelectrophiles. *Angew. Chem. Int. Ed*. **1993**, *32*, 767-788; b) Olah, G. A., Klumpp, D. A. Superelectrophiles and Their Chemistry. Wiley-VCH Verlag GmbH & Co. KGaA 2007.

2 Negishi, E. Principle of Activation of Electrophiles by Electrophiles through Dimeric Association—Two Are Better than One. *Chem. Eur. J*. **1999**, *5*, 411-420.

3 a) Albright, H.; Riehl, P. S.; McAtee. C. C. Reid, J. P.; Ludwig, J. R.; Karp, L. A.; Zimmerman, P. M.; Sigman, M. S.; Schindler, C.S. Catalytic Carbonyl-Olefin Metathesis of Aliphatic Ketones: Iron (III) Homodimers as Lewis Acidic Superelectrophiles. *J. Am. Chem. Soc.* **2019**, *141*, 1690-1700; b) Albright, H.; Vonesh, H. L.; Schindler, C. S. Superelectrophilic Fe(III)-Ion Pairs as Stronger Lewis Acid Catalysts for (*E*)-Selective Intermolecular Carbonyl-Olefin Metathesis. *Org. Lett.* **2020**, *22*, 3155-3160; c) Davis, A. J.; Watson, R. B.; Nasrallah, D. J.; Gomez-Lopez, J. L.; Schindler, C. S. Superelectrophilic Aluminium(III)–ion pairs promote a distinct reaction path for carbonyl–olefin ring-closing metathesis. *Nature Catal*. **2020**, *3*, 787-796.

4 Djurovic, A.; Vayer, M.; Li, Z.; Guillot, R.; Baltaze, J.-P.; Gandon, V.; Bour, C. Synthesis of Medium-Sized Carbocycles by Gallium-Catalyzed Tandem Carbonyl-Olefin Metathesis/Transfer Hydrogenation. *Org. Lett*. **2019**, *21*, 8132-8137.

5 Yang, S.; Bour, C.; Gandon, V. Superelectrophilic Gallium(III) Homodimers in Gallium Chloride Mediated Methylation of Benzene: a Theoretical Study. *ACS Catal*. **2020**, *10*, 3027-3033.

6 Evans, D. A.; Chapman, K. T.; Bisaha, J. Asymmetric Diels-Alder Cycloaddition Reaction with Chiral α,β-unsaturated N-Acyloxazolidinones. *J. Am. Chem. Soc.* **1988**, *110*, 1238-1256.

7 a) Bonnesen, P. V.; Puckett, C. L.; Honeychuck, R. V.; Hersh, W. H. Catalysis of Diels-Alder Reactions by Low Oxidation State Transition-Metal Lewis Acids: Fact and Fiction. *J. Am. Chem. Soc*. **1989**, *111*, 6070-6081; b) Bour, C.; Monot, J.; Tang, S.; Guillot, R.; Farjon, J.;

Gandon, V. Structure, Stability, and Catalytic Activity of the Fluorine-Bridged Complexes IPr·$GaCl_2$(μ-F)EF_{n-1} [EF_n^- = SbF_6^-, PF_6^-, BF_4^-]. *Organometallics*, **2014**, *33*, 594-599.

8 a) Wabnitz, T. C.; Yu, J.-Q.; Spencer, J. B. Evidence That Protons Can Be the Active Catalysts in Lewis Acid Mediated Hetero-Michael Addition Reactions. *Chem. Eur. J*. **2004**, *10*, 484-493; b) Dang, T. T.; Boeck, F.; Hintermann, L. Hidden Brønsted Acid Catalysis: Pathways of Accidental or Deliberate Generation of Triflic Acid from Metal Triflates. *J. Org. Chem*. **2011**, *76*, 9353-9361; c) Schmidt, R. K.; Müther, K.; Mück-Lichtenfeld, C.; Grimme, S.; Oestreich, M. Silylium Ion-Catalyzed Challenging Diels−Alder Reactions: The Danger of Hidden Proton Catalysis with Strong Lewis Acids. *J. Am. Chem. Soc*. **2012**, *134*, 4421-4428; d) Munz, D.; Webster-Gardiner, M.; Fu, R.; Strassner, T.; Goddard, III, W. A.; Gunnoe, T. B. Proton or Metal? The H/D Exchange of Arenes in Acidic Solvents. *ACS Catal.* **2015**, *5*, 769-775; e) Bour, C.; Guillot, R.; Gandon, V. First Evidence for the Existence of Hexafluoroantimonic(V) Acid. *Chem. Eur. J*. **2015**, *21*, 6066-6069; f) Šolić, I.; Lin, H. X.; Bates, R. W. Testing the Veracity of Claims of Lewis Acid Catalysis. *Tetrahedron Lett*. **2018**, *59*, 4434-4436.

9 a) Nakashima, D.; Yamamoto, H. Reversal of Chemoselectivity in Diels−Alder Reaction with α,β-Unsaturated Aldehydes and Ketones Catalyzed by Brønsted Acid or Lewis Acid. *Org. Lett.* **2005**, *7*, 1251-1253; b) Vayer, M.; Guillot, R.; Bour, C.; Gandon, V. Revealing the Activity of π-Acid Catalysts Using a 7-Alkynyl Cycloheptatriene. *Chem. Eur. J*. **2017**, *23*, 13901-13905.

10 S. Kobayashi, S. Nagayama, T. Busujima, Lewis Acid Catalysts Stable in Water. Correlation between Catalytic Activity in Water and Hydrolysis Constants and Exchange Rate

Constants for Substitution of Inner-Sphere Water Ligands. *J. Am. Chem. Soc.* **1998**, *120*, 8287-8288.

11 Williams, D. B. G.; Lawton, M. Metal triflates: On the Question of Lewis versus Brønsted Acidity in Retinyl Carbocation Formation. J. *Mol. Catal. A*, **2010**, *317*, 68-71.

12 Brown, H. C.; Kanner, E. Preparation and Reactions of 2,6-Di-t-butylpyridine and Related Hindered Bases. A Case of Steric Hindrance toward the Proton. *J. Am. Chem. Soc*. **1966**, *88*, 986-992.

13 a) Taylor, J. G.; Adrio, L. A.; Hii (Mimi), K. K. Hydroamination Reactions by Metal Triflates: Brønsted Acid vs. Metal Catalysis? *Dalton Trans*. **2010**, *39*, 1171-1175; b) Stereochemistry and Mechanism of the Brønsted Acid Catalyzed Intramolecular Hydrofunctionalization of an Unactivated Cyclic Alkene. McKinney Brooner, R. E.; Widenhoefer, R. A. *Chem. Eur. J*. **2011**, *17*, 6170-6178

14 Some protons may arise from elementary steps involving proton transfer in the catalytic cycle, while the presence of a hindered base in the reaction medium may, see: LaLonde, R. L.; Brenzovich Jr., W. E.; Benitez, D.; Tkatchouk, E.; Kelley, K.; Goddard III, W. A.; Toste, F. D. Alkylgold complexes by the intramolecular aminoauration of unactivated alkenes. *Chem. Sci*. **2010**, *1*, 226-233.

15 Lichtenthaler, M. R.; Stahl, F.; Kratzert, D.; Benkmil, B.; Wegner, H. A.; Krossing, I. σ- or π-Coordination? Complexes of Univalent Gallium Salts with Aromatic Nitrogen Bases. *Eur. J. Inorg. Chem.* **2014**, 4335-4341.

16 Ollevier, T.; Nadeau, E. Bismuth Triflate-Catalyzed Three-Component Mannich-Type Reaction. *J. Org. Chem*. **2004**, *69*, 9292-9295.

17 a) Li, H.-J.; Guillot, R.; Gandon, V. A Gallium-Catalyzed Cycloisomerization/Friedel–Crafts Tandem. *J. Org. Chem*. **2010**, *75*, 8435-8449; b) Tang, S.; Monot, J.; El-Hellani, A.; Michelet, B.; Guillot, R.; Bour, C.; Gandon, V. Cationic Gallium(III) Halide Complexes: a New Generation of π-Lewis Acids. *Chem. Eur. J*. **2012**, *18*, 10239-1024; c) Michelet, B.; Thiery, G.; Bour, C.; Gandon, V. On the Non-Innocent Behavior of Substrate Backbone Esters in Metal-Catalyzed Carbocyclizations and Friedel-Crafts Reactions of Enynes and Arenynes. *J. Org. Chem*. **2015**, *80*, 10925-10938; d) Michelet, B.; Tang, S.; Thiery, G.; Monot, J.; Li, H.; Guillot, R.; Bour, C.; Gandon, V. Catalytic Applications of [IPr·GaX_2][SbF_6] and Related Species. *Org. Chem. Front.* **2016**, *3*, 1603-1613; e) Li, Z.; Thiery, G.; Lichtenthaler, M. R.; Guillot, R.; Krossing, I.; Gandon, V.; Bour, C. Catalytic Use of Low-Valent Cationic Gallium(I) Complexes as π-Acids. *Adv. Synth. Catal*. **2018**, *360*, 544-549.

18 See inter alia: a) Willis, M. C. Transition Metal Catalyzed Alkene and Alkyne Hydroacylation. *Chem. Rev*. **2010**, 110, 725-748; b) Kacprzak, K.; Skiera, I.; Piasecka, M.; Paryzek, Z. Alkaloids and Isoprenoids Modification by Copper(I)-Catalyzed Huisgen 1,3-Dipolar Cycloaddition (Click Chemistry): Toward New Functions and Molecular Architectures. *Chem. Rev.* **2016**, *116*, 5689-5743; c) Tiwari, V. K.; Mishra, B. B.; Mishra, K. B.; Mishra, N.; Singh, A. S.; Chen, X. Cu-Catalyzed Click Reaction in Carbohydrate Chemistry. *Chem. Rev*. **2016**, *116*, 3086-3240.

19 Dong, Z.; Ren, Z.; Thompson, S. J.; Xu, Y.; Dong, G. Transition-Metal-Catalyzed C–H Alkylation Using Alkenes. *Chem. Rev*. **2017**, *117*, 9333-9403.

20 a) Weaver, J. D.; Recio, A.; Grenning, A. J.; Tunge, J. A. Transition Metal-Catalyzed Decarboxylative Allylation and Benzylation Reactions. *Chem. Rev*. **2011**, *111*, 1846-1913; b) Mishra, N. K.; Sharma, S.; Park, J.; Han, S.; Kim, I. S. Recent Advances in Catalytic C(sp^2)–H Allylation Reactions. *ACS Catal.* **2017**, *7*, 2821-2847; c) Messinis, A. M.; Finger, L. H.; Hu, L.; Ackermann, L. Allenes for Versatile Iron-Catalyzed C–H Activation by Weak O-Coordination: Mechanistic Insights by Kinetics, Intermediate Isolation, and Computation. *J. Am. Chem. Soc*. **2020**, *142*, 13102-13111.

21 a) Nishibayashi, Y.; Yoshikawa, M.; Inada, Y.; Hidai, M.; Uemura, S. Ruthenium-Catalyzed Propargylation of Aromatic Compounds with Propargylic Alcohols. *J. Am. Chem. Soc.* **2002**, *124*, 11846-11847; b) Nishibayashi, Y.; Inada, Y.; Yoshikawa, M.; Hidai, M.; Uemura, S. Propargylation of Aromatic Compounds with Propargylic Alcohols Catalyzed by a Cationic Diruthenium Complex. *Angew. Chem. Int. Ed.* **2003**, *42*, 1495-1498; c) Kennedy-Smith, J. J.; Young, L. A.; Toste, F. D. Rhenium-Catalyzed Aromatic Propargylation. *Org. Lett.* **2004**, *6*, 1325-1327; d) Sanz, R.; Martínez, A.; Álvarez-Gutiérrez, J. M.; Rodríguez, F. Metal-Free Catalytic Nucleophilic Substitution of Propargylic Alcohols. *Eur. J. Org. Chem.* **2006**, 1383-1386; e) Matsuzawa, H.; Miyake, Y.; Nishibayashi, Y. Ruthenium-Catalyzed Enantioselective Propargylation of Aromatic Compounds with Propargylic Alcohols via Allenylidene Intermediates *Angew. Chem. Int. Ed*. **2007**, *46*, 6488-6491; f) Ding, C.-H.; Hou, X.-L. Catalytic Asymmetric Propargylation. *Chem. Rev*. **2011**, *111*, 1914-1937; g) McCubbin, J. A.; Nassar, C.;

Krokhin, O. V. Waste-Free Catalytic Propargylation/Allenylation of Aryl and Heteroaryl Nucleophiles and Synthesis of Naphthopyrans. *Synthesis* **2011**, 3152-3160;

22 a) Wu, S.; Huang, X.; Wu, W.; Li, P.; Fu, C.; Ma, S. A C–H Bond Activation-Based Catalytic Approach to Tetrasubstituted Chiral Allenes. *Nat. Commun*. **2015**, *6*, 7946-7954; b) Lu, Q.; Greßies, S.; Klauck, F. J. R.; Glorius, F. Manganese(I)-Catalyzed Regioselective CH-Allenylation: DirectAccess to 2-Allenylindoles. *Angew. Chem. Int. Ed*. **2017**, *56*, 6660-6664; b) Wu, S.; Huang, X.; Wu, W.; Li, P.; Fu, C.; Ma, S. A C–H Bond Activation-Based Catalytic Approach to Tetrasubstituted Chiral Allenes. *Nat. Commun*. **2015**, *6*, 7946-7954.

23 a) Li, C.; Wang, J. Lewis Acid Catalyzed Propargylation of Arenes with O-Propargyl Trichloroacetimidates: Synthesis of 1,3-Diarylpropynes. *J. Org. Chem*. **2007**, *72*, 7431-7434; b) Yu, Y.-B.; Luo, Z.-J.; Zhang, X. Copper-Catalyzed Direct Propargylation of Polyfluoroarenes with Secondary Propargyl Phosphates. *Org. Lett.* **2016**, *18*, 3302-3305.

24 Zhu, C. C.; Schwarz, J. L.; Cembellín, S.; Greßies, S.; Glorius, F. Highly Selective Manganese(I)/Lewis Acid Cocatalyzed Direct C-H Propargylation Using Bromoallenes. *Angew. Chem. Int. Ed.* **2018**, *57*, 437-441.

25 a) Schade, M. A.; Yamada, S.; Knochel, P. Synthesis of Polyfunctional Allenes by Successive Copper-Mediated Substitutions. *Chem. Eur. J*. **2011**, *17*, 4232-4237; b) Deng, Y.; Bartholomeyzik, T.; Bäckvall, J.-E. Control of Selectivity in Palladium-Catalyzed Oxidative Carbocyclization/Borylation of Allenynes. *Angew. Chem. Int. Ed*. **2013**, *52*, 6283-6287.

26 a) Hoffmann-Röder, A.; Krause, N. Synthesis and Properties of Allenic Natural Products and Pharmaceuticals. *Angew. Chem. Int. Ed.* **2004**, *43*, 1196-1216; b) Ji, N.-Y.; Li, X.-M.; Wang, B.-G. Halogenated Terpenes and a C15-Acetogenin from the Marine Red Alga *Laurencia Saitoi*. *Molecules* **2008**, *13*, 2894-2899; c) Ji, N.-Y.; Li, X.-M.; Li, K.; Ding, L.-P.; Gloer, J. B.; Wang, B.- G. Diterpenes, Sesquiterpenes, and a C15-Acetogenin from the Marine Red Alga *Laurencia Mariannensis. J. Nat. Prod.* **2007**, *70*, 1901-1905; d) Alnafta, N.; Schmidt, J. P.; Nesbitt, C. L.; McErlean, C. S. P. Total Synthesis of (+)-Panacene. *Org. Lett.* **2016**, *18*, 6520-6522.

27 For selected examples, see: a) Ohno H.; Hamaguchi H.; Tanaka T. Stereoselective Synthesis of Chiral 2,3-*cis*-2-ethynylaziridines by Base-Mediated Intramolecular Amination of Bromo-Allenes. *Org. Lett*. **2001**, *3*, 2269-2271; b) Hamaguchi H.; Kosaka S.; Ohno H.; Tanaka T. Bromoallenes as Allyl Dication Equivalents in the Absence of Palladium(0): Synthesis of Bicy-clic Sulfamides by Tandem Cyclization of Bromoallenes. *Angew. Chem. Int. Ed*. **2005**, *44*, 1513-1517; c) Trost B. M.; Stiles D. T. Synthesis of Allenamides by Copper-Catalyzed Coupling of Allenyl Halides with Amides, Carbamates, and Ureas. *Org. Lett*. **2005**, *7*, 2117-2120; d) Xu. L.; Huang, X.; Zhong, F. Intermolecular Tandem Addition−Cyclization of Bromo-allenes: A Facile Synthesis of Methylenecyclopropyl Carboxylates and Polysubstituted Furans. *Org. Lett*. **2006**, *8*, 5061-5064; e) Tang C. J.; Wu Y. K. On the Synthesis of Cepacin A. *Tetrahedron*, **2007**, *63*, 4887-4906; f) Persson, A. K. Å.; Johnston, E. V.; Bäckvall, J.-E. Copper-Catalyzed N-Allenylation of Allylic Sulfonamides. *Org. Lett*. **2009**, *11*, 3814-3817; g) Woerly, E. M.; Cherney, A. H.; Davis, E. K.; Burke, M. D. Stereoretentive Suzuki−Miyaura Coupling of Haloallenes Enables Fully Stereocontrolled Access to (−)-Peridinin. *J. Am. Chem. Soc*. **2010**, *132*, 6941-6943.

28 Vayer, M.; Bour, C.; Gandon, V. Synthesis of 3-Substituted 3-Bromo-1-phenylallenes from Alkynylcycloheptatrienes. *J. Org. Chem*. **2018**, *83*, 11309-11317.

29 The reaction works equally well down to 40 °C, but we kept the temperature of 80 °C because other arenes are not reactive at 40 °C.

30 For an analogy between gallium and zinc halides in catalysis, see: Tian, J.; Chen, Y.; Vayer, M.; Djurovic, A.; Guillot, R.; Guermazi, R.; Dagorne, S.; Bour, C.; Gandon, V. Exploring the Limits of π-Acid Catalysis Using Strongly Electrophilic Main Group Metal Complexes: the case of Zinc and Aluminium. *Chem. Eur. J*. **2020**, *26*, 12831-12838.

31 McGarvey, B. R.; Taylor, M. J.; Tuck, D. G. Gallium-71 NMR Studies of Anionic Gallium Halide Species in Nonaqueous Solution. *Inorg. Chem*. **1981**, *20*, 2010-2013.

32 Casado, J.; Lopez-Quintela, M. A.; Lorenzo-Barral, F. M. The Initial Rate Method in Chemical Kinetics: Evaluation and Experimental Illustration. *J. Chem. Educ.* **1986**, *63*, No. 450-452.

33 Bures, J. A Simple Graphical Method to Determine the Order in Catalyst. *Angew. Chem. Int. Ed.* **2016**, *55*, 2028-2031.

34 Frisch, M. J.; Trucks, G. W.; Schlegel, H. B.; Scuseria, G. E.; Robb, M. A.; Cheeseman, J. R.; Scalmani, G.; Barone, V.; Mennucci, B.; Petersson, G. A.; Nakatsuji, H.; Caricato, M.; Li, X.; Hratchian, H. P.; Izmaylov, A. F.; Bloino, J.; Zheng, G.; Sonnenberg, J. L.; Hada, M.; Ehara, M.; Toyota, K.; Fukuda, R.; Hasegawa, J.; Ishida, M.; Nakajima, T.; Honda, Y.; Kitao, O.; Nakai, H.; Vreven, T.; Montgomery, J. A., Jr.; Peralta, J. E.; Ogliaro, F.; Bearpark, M.; Heyd, J. J.; Brothers, E.; Kudin, K. N.; Staroverov, V. N.; Kobayashi, R.; Normand, J.; Raghavachari, K.;

Rendell, A.; Burant, J. C.; Iyengar, S. S.; Tomasi, J.; Cossi, M.; Rega, N.; Millam, J. M.; Klene, M.; Knox, J. E.; Cross, J. B.; Bakken, V.; Adamo, C.; Jaramillo, J.; Gomperts, R.; Stratmann, R. E.; Yazyev, O.; Austin, A. J.; Cammi, R.; Pomelli, C.; Ochterski, J. W.; Martin, R. L.; Morokuma, K.; Zakrzewski, V. G.; Voth, G. A.; Salvador, P.; Dannenberg, J. J.; Dapprich, S.; Daniels, A. D.; Farkas, O.; Foresman, J. B.; Ortiz, J. V.; Cioslowski, J.; Fox, D. J. Gaussian 09, Revision D.01; Gaussian, Inc., Wallingford, CT, 2009.

35 Chai, J.-D.; Head-Gordon, M. Systematic Optimization of Long-range Corrected Hybrid Density Functionals. *J. Chem. Phys*. **2008**, *128*, 084106.

36 a) Krishnan, R.; Binkley, J. S.; Seeger, R.; Pople, J. A. Self-consistent Molecular Orbital Methods. XX. A basis Set for Correlated Wave Functions. *J. Chem. Phys.* **1980**, *72*, 650-654; b) McLean, A. D.; Chandler, G. S. Radom, L. Contracted Gaussian Basis Sets for Molecular Calculations. I. Second Row Atoms, Z=11–18. *J. Chem. Phys*. **1980**, *72*, 5639-5648; c) Blaudeau, J.-P.; McGrath, M. P.; Curtiss, L. A. Extension of Gaussian-2 (G2) Theory to Molecules Containing Third-row Atoms K and Ca. *J. Chem. Phys.* **1997**, *107*, 5016-5021; d) Curtiss, L. A.; McGrath, M. P.; Blandeau, J.-P.; Davis, N. E.; Binning, R. C.; Radom, Jr. L. Extension of Gaussian-2 Theory to Molecules Containing Third‐row Atoms Ga‐Kr. *J. Chem. Phys.* **1995**, *103*, 6104-6113; e) Glukhovstev, M. N.; Pross, A.; McGrath, M. P.; Radom, L. Extension of Gaussian-2 (G2) Theory to Bromine- and Iodine-containing Molecules. Use of Effective Core Potentials. *J. Chem. Phys*. **1995**, *103*, 1878-1885.

37 a) Tomasi, J.; Mennucci, B.; Cammi, R. Quantum Mechanical Continuum Solvation Models. *Chem. Rev*. **2005**, *105*, 2999-3093; b) Scalmani G.; Frisch, M. J. Continuous Surface

Charge Polarizable Continuum Models of Solvation. I. General Formalism. *J. Chem. Phys*. **2010**, *132*, 114110-11415.

38 a) Fischer, W.; Jübermann, O. Über Thermische Eigenschaften von Halogeniden. Dampfdrucke und Dampfdichten von Gallium III-Halogeniden. *Z. Anorg. Allg. Chem*. **1936**, *227*, 227-236; b) Laubengayer A. W.; Schirmer, F. B. The Chlorides of Gallium. *J. Am. Chem. Soc*. **1940**, *62*, 1578-1583.

39 Černý, Z.; Macháček, J.; Fusek, J.; Čásenský, B.; Kříž, O.; Tuck, D. G. Multinuclear NMR Studies of Mixtures of Aluminium and Gallium Trihalides in Benzene. *J. Chem. Soc., Dalton Trans*. **2001**, 2698-2703.

40 The formation of the ion pair from **1a** and 0.5 Ga_2Cl_6 liberates 5.5 kcal/mol in Scheme 6, Eq 12 (3.3 + 2.2 kcal/mol) and not 3.8 kcal/mol. This difference comes from the fact that anisole is explicitly present in Scheme 8, so **B** is a 3-component adduct.

41 This 1,4-addition is not possible using the $GaCl_3Br^-$ ion as a Cl^- or Br^- nucleophile.

42 a) Olah, G. Mechanism of Electrophilic Aromatic Substitutions. *Acc. Chem. Res*. **1971**, *4*, 240-248; b) Backstrom, N.; Burton, N. A.; Turega, S.; Watt, I. F. The Primary Kinetic Hydrogen Isotope Effect in the Deprotonation of a Nitroalkane by an Intramolecular Carboxylate Group. *J. Phys. Org. Chem*. **2008**, *21*, 603-613.

TOC

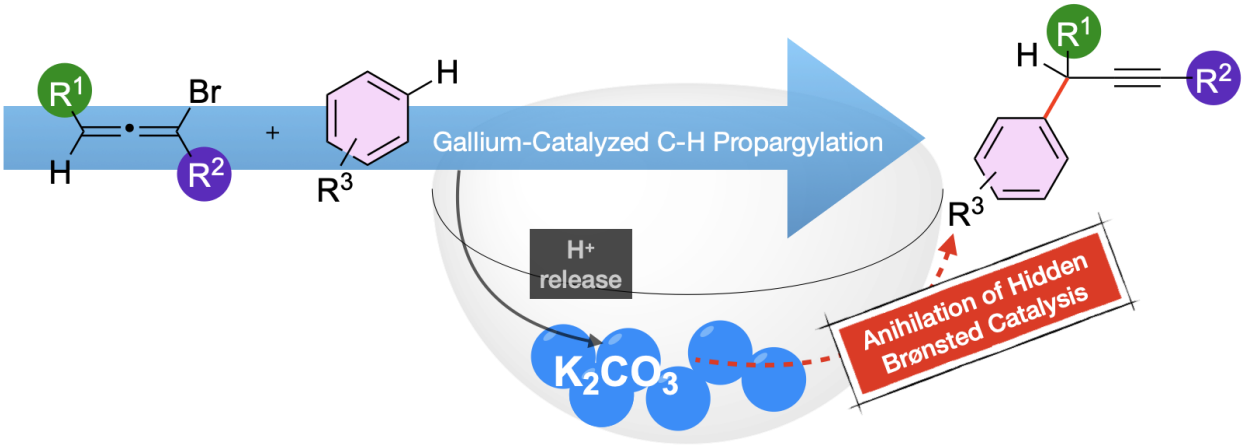

selective C-H propargylation with Gallium
valuable allenes, chemoselective
detailed mechanisitic studies: kinetics, computations